https://doi.org/10.1016/j.ijheatmasstransfer.2015.01.046

Effects of geometrical parameters on the thermohydraulic characteristics of periodic cross-corrugated channels

X.P. Liu[1], J.L. Niu[1,*]

[1] Department of Building Services Engineering, The Hong Kong Polytechnic University, Hong Kong

[*]Corresponding author. Tel: (852) 2766 7781; fax: (852) 2774 6146.

E-mail address: bejlniu@polyu.edu.hk

Abstract

Simulations are performed to study the geometric effect on thermohydraulic characteristics of a periodic cross-corrugated channel for the Re range of 200-3000. The effect of apex angle and aspect ratio on heat transfer, pressure drop and thermohydraulic performance in the corrugated channel is investigated. To accurately predict the transitional flow in the topology, a model performance evaluation is conducted in two steps through the cross comparisons between predictions and related correlations (or experiment results). Of the seven turbulence models selected, the Reynolds stress model fits the correlation and experiment the best and thus is employed for comparative study. The results show that the Apex angle strongly influence the heat transfer and pressure loss in a triangular cross-section corrugated channel. For the purpose of heat transfer enhancement, cross-corrugated triangular channels at the 90°and 120° Apex angles are recommended. The aspect ratio has a relatively greater impact on flow frictional loss, compared to its effect on the heat transfer for the studied cases. For this flow regime, the cross-corrugated triangular duct with the Apex angle of 150° is shown to be the optimum choice over all the studied channels. The JF factor is enhanced by 4.1 to 7.0 times that in a triangular channel with Apex angle of 90°.

Keywords

Heat transfer enhancement, Geometric effect, Cross-corrugated channel

1. Introduction

In recent years, energy crisis and the thrust for energy conservation have driven the development for high efficiency heat exchangers. The demand for economical, high performance, space saving and lightweight heat exchangers has influenced the research of compact surfaces. Compact heat exchangers characterised by high heat transfer surface area to volume ratios have received great attention due to its high heat transfer coefficients compared to other exchanger types [1].

Cross-corrugated channels are the basic channel geometry in plate heat exchangers and are widely used in many applications such as electronic cooling, spacecraft, air conditioning, refrigeration, and so on. It has passive enhancement of the heat transfer process where secondary flow structures are created by means of corrugated surfaces. Recently, with the development of membrane technologies, cross-corrugated channels have also attracted attention in membrane-related industries such as membrane energy recovery [2]. In such applications, both the heat and mass transfer in the duct and in the membrane itself are important. From material side, encouraging results are emerging with the introduction of new materials that can offer heat and moisture recovery at the same time [3-5]. From duct side, the use of cross-corrugated exchangers has been proven to increase the mechanical strength of the plates as well as the heat transfer rate [6]. The configuration is shown in Figure. 1, where two unmixed cross flows exchange heat through corrugated plates. Flat membrane sheets are corrugated to form a series of parallel ducts. Sheets of the corrugated plates are then stacked together to form a 90°orientation angle between the neighbouring plates, which guarantees the same flow pattern for both fluids. With a pre-designed plastic frame, corrugated duct walls are formed to support the ultrathin membranes and construct the required geometry.

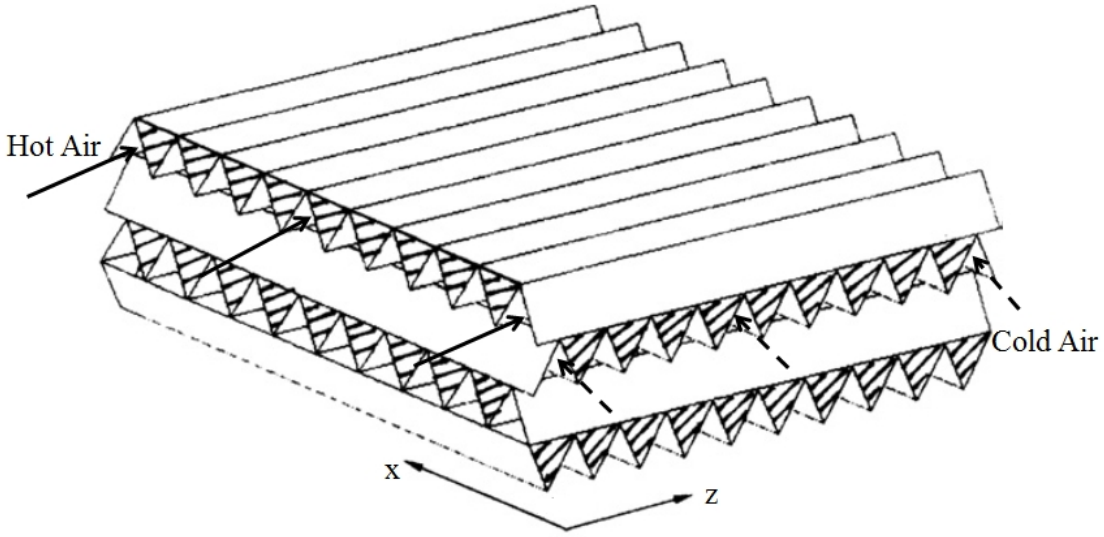

Fig.1 Schematic of the cross-corrugated exchanger applied in heat recovery application

Flow and heat transfer in corrugated channels are complicated and strongly influenced by the geometrical parameters, including the inclination angle and the corrugation profile of the channels. Many studies have been carried out to investigate the forced convection flow in corrugated channels by means of experimental and numerical approaches. Focke et al. [7] experimentally investigated the effect of the corrugation inclination angle on the thermo-hydraulic performance of the heat exchanger through the use of the electrochemical mass transfer analogy. They found that a 90° orientation angle produces the largest driving force that generates swirl in the furrows. Satisk et al. [8] carried out experimental studies to illustrate the geometry effect on the heat transfer and pressure drop of corrugated passages. Muley and Manglik [9] conducted a series of tests to study the thermohydraulic performance of the corrugated plate with different plate configurations. Zimmerer et al. [10] studied the effects of the inclination angle, the wavelength, the amplitude and the shape of the corrugation on the heat and mass transfer of the exchanger. These experimental studies identified that the geometrical parameters have significant effect on the thermohydraulic characteristics of the exchangers.

In addition to these experimental studies, extensive effort has been made to numerically investigate thermohydraulic characteristics of the corrugated channels [11-12]. Compared with

experimental method, computational fluid dynamics (CFD) method is an effective and economical tool for obtaining detailed flow structures between corrugated plates and is widely used in comparative studies. Before investigating geometric effects on the thermohydraulic characteristics in the cross-corrugated channels, the reliability and computational cost of using the numerical method should be evaluated. It is of essential importance to accurately reproduce the flow features and the hydrothermal behaviour. It is generally agreed that the flow inside the corrugation plates has an earlier transition to turbulent flow than that of conventional parallel plates [12]. Laminar flow model would not serve as an appropriate viscous model for simulating the flow in corrugated channels. The choice of the most suitable turbulence model is essentially the key to successfully modelling the complex flow in the channel. Ciofalo et al. [11] compared the use of different viscous models in the Reynolds number range between 1000 and 10000. They found that Standard $k-\varepsilon$ model with standard wall functions is completely inapplicable at low Re. Kanaris et al. [13] examined the ability of a general purpose CFD code to predict the flow and heat transfer characteristics in a corrugated channel. A two-equation turbulence model (SST) is used and the simulations are conducted for a Reynolds number range from 400 to 1400. Zhang and Che [14] performed numerical predictions of fluid flow and heat transfer between cross-corrugated plates. Results predicted by eight turbulence models were compared with available experimental data for the purpose of model performance evaluation. Han et al. [15] briefly reviewed the viscous models used in the previous investigations of fluid flowing in corrugated plates, and it was found that the most appropriate viscous model is still an open issue. On the other hand, the use of CFD method allows computation for various geometrical configurations in order to evaluate their effects, during which the computational cost cannot be overlooked. Some researchers simulated the fluid flowing between the whole cross-corrugated plates [13]. Tsai et al. [16] numerically investigated the hydrodynamic characteristics and distribution of flow in two real-size cross-corrugated channels. However, it results in an increase of computational cost, which is not desired in comparative studies and optimization analysis. An alternative method is using a single cell as the computational domain, which is the smallest and repeated element in the cross-corrugated channels [11] [12] [17-19]. Periodicity is used to reduce the complexity of channel geometry and enables the smallest possible segment of the flow channel to be modelled. A considerable amount of computational cost could be saved by utilizing the unitary cell.

For the novel cross-corrugated channels used in membrane recovery application, with corrugation angle of 90° between two neighboring plates, the duct geometry is expected to influence the flow and heat transfer capacity of the exchanger. Shah and London [20] studied the heat transfer characteristics of laminar flow in a wide variety of channel shapes for an extensive range of thermal boundary conditions. Besides the sinusoidal cross-section ducts that usually used in metal plate heat exchangers, there have been several reports on heat transfer and friction characteristics in channels with other-shaped cross-sections, such as semi-circular, triangular and trapezoidal shapes. Zheng et al. [21] numerically studied the flow and heat transfer characteristics of channels with a semi-circular cross-section in the laminar flow regime for different Reynolds numbers and Prandtl numbers. Leung and Probert [22] experimental investigate the thermal behaviours of turbulent air-flows through triangular passages in compact heat-exchangers with three different apex-angles. Chen et al. [23] studied numerically the flow and heat transfer characteristics of smooth triangular ducts with different apex angles for fully-developed laminar flow conditions. Gupta et al. [24] performed simulations to study the heat transfer behaviour of an equilateral triangular section duct for fully-developed laminar flows with Reynolds numbers below 200. Wu and Cheng [25] measured the friction factor of laminar flow of deionized water in smooth silicon microchannels of trapezoidal cross-section. The results showed that the friction constant of these microchannels is greatly influenced by the cross-sectional aspect ratio, which is defined as the ratio of small base to big base of the trapezoid. McHale et al. [26] numerically studied the heat transfer in the thermal entrance region of trapezoidal microchannels. The effects of sidewall angle and the aspect ratio (small base of trapezoid to channel height) upon the local and average heat transfer coefficients in the trapezoidal duct are explored. These previous studies illustrated that the cross-section shape of the channel is a major parameter in influencing the thermohydraulic characteristics of heat exchangers. However, such geometric effect on flow and heat transfer in the novel cross-corrugated channels used in membrane recovery application has not been studied previously.

The present study is aimed to numerically investigate the geometrical effect on the thermohydraulic characteristics of periodic cross-corrugated channels in typical transitional flow regime with Reynolds number between 200-3000. Yang et al. [27] investigated the transitional

flow and heat transfer in periodic fully developed corrugated duct in the Reynolds number range of 100 to 2500, while Zhang [28] examined the flow structure and heat transfer characteristics in a periodically fully developed cross-corrugated duct in transitional flow regime between Re=100 and 6000. By comparison, very little work has been undertaken on the duct geometry effects on the thermohydraulic characteristics in this flow regime. In this paper, the effect of apex angle and aspect ratio upon thermohydraulic characteristics of the corrugated channel is explored. This study covers a wide range of apex angles from 30° to 150° for isosceles triangular cross-section channel, and the cross-sectional aspect ratios (small base to big base of the trapezoid) from 0.2 to 0.6 for isosceles trapezoidal cross-section ducts. The results of this study would be helpful for the design and optimization of cross-corrugated heat exchangers.

2. Method and Models

2.1 Computational domain and Problem formulation

For the cross-corrugated channel geometry described in Figure 1, constant property, periodically developed flows are considered. In ducts with periodically varying flow cross-section or wall geometry in the streamwise direction, the concept of periodically developed flow, as treated by Patankar et al. [29], is applicable. Figure 2 shows the unitary cells used for CFD modelling. The apex angle of isosceles triangular cross-section channel and the sidewall angle of isosceles trapezoidal cross-section channel are also depicted in the figure. For the channel with trapezoidal cross-section, the cross-sectional aspect ratio is defined as B/L.

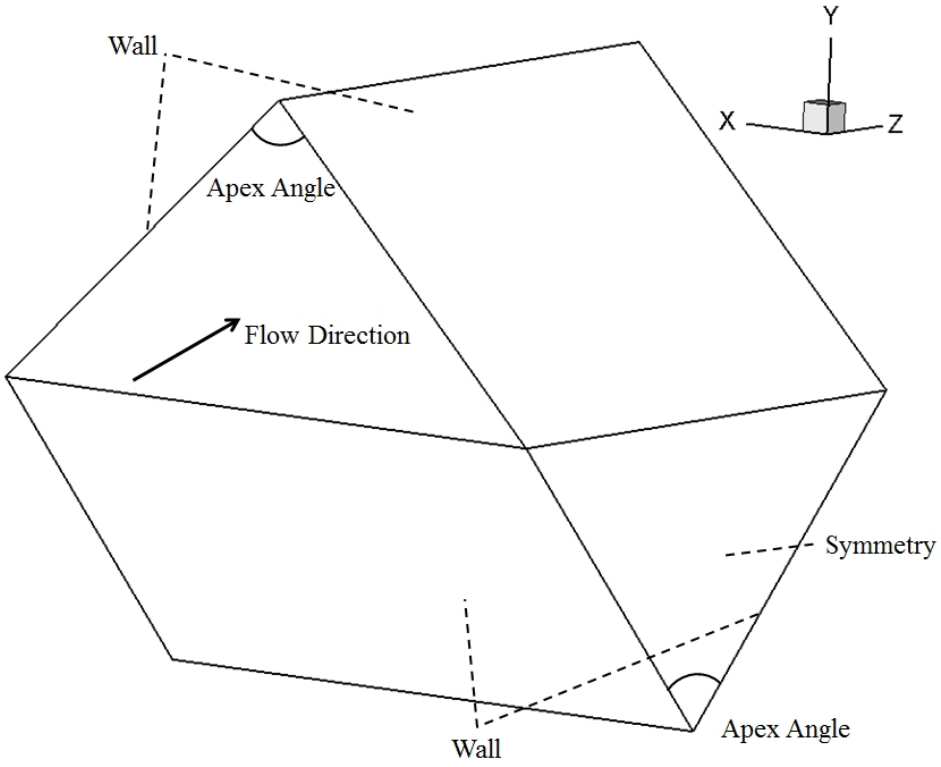

(a)

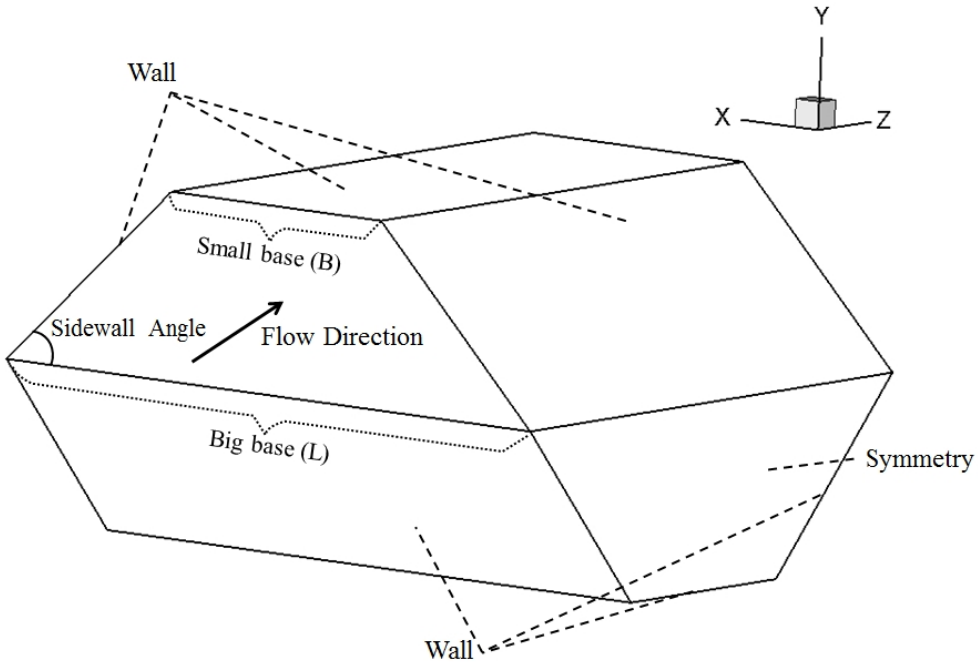

(b)

Fig.2 Unitary cells used for CFD modelling and the boundary conditions. (a) Triangular cross-section (Apex angle = 90°), (b) Trapezoidal cross-section (B/L = 0.4, Sidewall angle = 45°)

The hydraulic diameter of the channel is defined as

$$D_h = \frac{4V_t}{A_t} \tag{5}$$

where V_t is the volume of the unit cell and A_t is wetted surface area. To focus on the effect induced by different cross-section shapes, constant D_h is used for all the studied plates here. Detailed geometrical data of the studied plates are summarized in Table 1.

Tab.1 Detailed geometrical data of different cross-corrugated plates

		V_t	A_t	D_h	L_i	A_{in}
Triangular Cross-section	Apex=30°	2.071E-06	8.282E-04	1.000E-02	1.035E-02	1.000E-04
	Apex=60°	1.333E-06	5.333E-04	1.000E-02	1.155E-02	5.774E-05
	Apex=90°	1.414E-06	5.657E-04	1.000E-02	1.414E-02	5.000E-05
	Apex=120°	2.309E-06	9.238E-04	1.000E-02	2.000E-02	5.774E-05
	Apex=150°	7.727E-06	3.091E-03	1.000E-02	3.864E-02	1.000E-04
Trapezoidal Cross-section (Sidewall angle= 45°)	B/L=0.2	1.280E-06	5.121E-04	1.000E-02	1.387E-02	4.616E-05
	B/L=0.4	1.379E-06	5.517E-04	1.000E-02	1.486E-02	4.639E-05
	B/L=0.6	1.934E-06	7.734E-04	1.000E-02	1.821E-02	5.308E-05
Trapezoidal Cross-section (Sidewall angle= 30°)	B/L=0.2	2.310E-06	9.239E-04	1.000E-02	2.028E-02	5.696E-05
	B/L=0.4	2.774E-06	1.110E-03	1.000E-02	2.253E-02	6.156E-05
	B/L=0.6	4.385E-06	1.754E-03	1.000E-02	2.874E-02	7.629E-05

The Reynolds number, Re, is defined as

$$Re = \frac{\rho u_m D_h}{\mu} \tag{9}$$

where u_m is the inlet velocity (m s^{-1}), μ is air dynamic viscosity (kg m^{-1} s^{-1}), ρ is the density of air (kg m^{-3}).

The cycle-average heat transfer coefficient is obtained from the temperature difference between the inlet and the outlet of a unitary cell,

$$h = \frac{\rho u_m A_{in} c_p (T_{fo} - T_{fi})}{A_t \Delta T_{\lg}}$$

where A_{in} is the inlet area of the unit cell (m^2), c_p is specific heat of air (kJ kg^{-1} K^{-1})), $\Delta T_{\lg}$ is the log mean temperature difference between the wall and fluid, which is

$$\Delta T_{\lg} = \frac{(T_{fi} - T_w) - (T_{fo} - T_w)}{\ln(T_{fi} - T_w)/(T_{fo} - T_w)} \tag{3}$$

where subscripts " f, w, i, o " refer to "air, wall, inlet and outlet" respectively.

The Nusselt number can be calculated by

$$Nu = \frac{hD_h}{\lambda} \tag{4}$$

where λ is air conductivity (kW m^{-1} K^{-1}).

The Stanton number *St* and Colburn j -factor is then calculated by

$$St = \frac{Nu}{RePr}$$

$$j = StPr^{-2/3}$$

The Fanning friction factor f is calculated by

$$f = \frac{(\Delta p / L_i) D_h}{2\rho u_m^2}$$

where L_i is the length of a unitary cell (m), Δp is the pressure difference between the inlet and outlet of a cell (Pa).

2.2 Numerical procedures:

Due to the small characteristic length of the studied passages, the Reynolds numbers are in the range of 200–3000, and the flow is in transitional flow regime [18]. In the present study, the turbulence effect in this regime is modelled with turbulence models. The incompressible flow is described by conservation of mass (the continuity equation), momentum (Navier-Stokes equation), and energy (the temperature equation for the fluid).The Reynolds-averaged approach represents transport equations for the mean flow quantities only, with all the scales of the

turbulence being modelled. For constant air properties, the steady-state Reynolds-averaged governing equations can be summarized as follows:

$$\frac{\partial}{\partial x_i}(\rho u_i) = 0$$

$$\frac{\partial}{\partial x_j}(\rho u_i u_j) = -\frac{\partial p}{\partial x_i} + \frac{\partial}{\partial x_j}\left[\mu(\frac{\partial u_i}{\partial x_j} + \frac{\partial u_j}{\partial x_i}) - \rho\overline{u_i' u_j'}\right]$$

$$\frac{\partial}{\partial x_i}(\rho C_p u_i T) = -\frac{\partial}{\partial x_i}\left(-k\frac{\partial T}{\partial x_i} + \rho C_p \overline{u_i' T'}\right)$$

where subscripts (i and j) represent the tensor notation (i=1,2,3 and j=1,2,3). u_i, p and T represent the velocity vector, pressure and temperature, respectively. ρ, μ, k and C_p represent the fluid density, viscosity, thermal conductivity and specific heat. Additional turbulence model is necessary to close the equations due to more than five unknown variables exist in these equations.

Standard $k-\varepsilon$ model (Ske) [30], RNG $k-\varepsilon$ model (RNG) [31], realizable $k-\varepsilon$ model (RLZ) [32], shear-stress transport $k-\omega$ model (sst-kw) [33], Transition shear-stress transport model (Trans-sst) [34], $k-kl-\omega$ model (k-kl-w) [35] and Reynolds stress model (RSM) [36] are selected in this study for for the purpose of model performance evaluation. The first four models are well-known two-equation models that have been widely used for many engineering applications. The transition SST model is based on the coupling of the SST $k-\omega$ transport equations with two other transport equations, one for the intermittency and one for the transition onset criteria, in terms of momentum-thickness Reynolds number. The $k-kl-\omega$ model was developed to predict boundary layer development and calculate transition onset. It is considered to be a three-equation type model, which includes transport equations for turbulent kinetic energy, laminar kinetic energy, and the inverse turbulent time scale. Abandoning the isotropic eddy-viscosity hypothesis, the RSM model closes the Reynolds-averaged Navier-Stokes equations by solving transport equations for the Reynolds stresses, together with an equation for the dissipation rate. This means that seven additional transport equations are solved in three-dimensional flow. All the values of y^+ on the wall surfaces are less than 5 based on the preliminary computational results applying standard $k-\varepsilon$ model. Thus the enhanced wall

treatment [37], which is a near-wall model approach that combines a two-layer model with enhanced wall functions, can be used for Ske, RNG, RLZ and RSM models. It should be noted that when RSM is applied to near-wall flows using the enhanced wall treatment in ANSYS FLUENT, the linear pressure-strain model needs to be modified [37]. In view of the limitation of paper length, detailed equations of the turbulence models are not listed, and can be found in the related references.

The SIMPLEC scheme was used for the pressure-velocity coupling, and the second-order upwind scheme based on the finite volume method was adopted for the spatial discretization. Considering the geometrical nature of the unitary cell, the computational domain is meshed with triangular prism grids in order to reduce the computational cost. The meshes were carefully examined to avoid unsatisfied skewness which could lead to convergence difficulties and inaccuracies in the numerical solution. The boundary conditions considered in the present simulations were shown in Figure 2. The upper and lower walls were set to the ordinary no-slip conditions. Uniform wall temperature conditions are employed as thermal boundary conditions. Periodic boundary conditions were imposed in the flow direction for the computational domain of a unitary cell. At both sides of the domain, the symmetry type conditions were used. A prescribed mass flow rate in the flow direction was specified. In the present study, the flow field and heat transfer were calculated separately since the temperature is assumed to be a passive scalar when the buoyancy effect is neglected. The residuals, together with mean pressure and temperature gradient were monitored to identify convergence. Convergence is assumed to be obtained when the scaled residuals [37] of all the governing equations reach 10^{-5}, with an exception for the residuals of energy equation reach 10^{-8}. The convergence becomes more difficult for large Re, where smaller relax factors were used. Normally more than 6000 iterations are required before a satisfactory convergence is achieved.

3. Results and Discussions

3.1 Models Validation

Before starting numerical investigation on the geometrical effect, it is necessary to find the most suitable turbulence model to accurately predict the complex flow in the channel. The performance of seven turbulence models (Ske, RNG, RLZ, sst-kw, Trans-sst, k-kl-w and RSM models) for simulating flow and heat transfer in transitional duct flow is quantitatively evaluated here. The model performance evaluation is conducted in two steps. Firstly, the heat transfer and fluid flow in a straight triangular duct is numerically studied. The laminar, transition and fully turbulent region for such classical geometry is well known, and the prediction results are compared with the related correlation results in the transitional flow regime. Thus the performance of different turbulence models for simulating the convective flow in a triangular duct in the transition region can be assessed. Secondly, based on this preliminary comparison, selected models are employed for further evaluation. Comparisons are made between the prediction and experimental data, which was obtained in a cross-corrugated triangular channel. Same geometry and grid are used during the evaluation process to provide comparison only of the model performance.

For the flow and heat transfer in triangular duct, the errors of using Dittus-Boelter equation may be as large as 25%. Such errors can be reduced to less than 10% through the use of more recent, but generally more complex correlations. In order to get a higher level of accuracy, the correlation used is as follows, provided by Gnielinski ($3000 \le Re_D \le 5\times10^6$, including the transition region $2300 < Re_D < 10^4$) [38]

$$Nu = \frac{(f_D/8)(Re_D - 1000)Pr}{1+12.7(f_D/8)^{1/2}(Pr^{2/3}-1)}$$

where the friction factor is obtained from the correlation developed by Petukhov:

$$f_D = (0.790\ln Re_D - 1.64)^{-2}$$

It should be noted that f_D is the Darcy friction factor, which is four times of the Fanning friction factor.

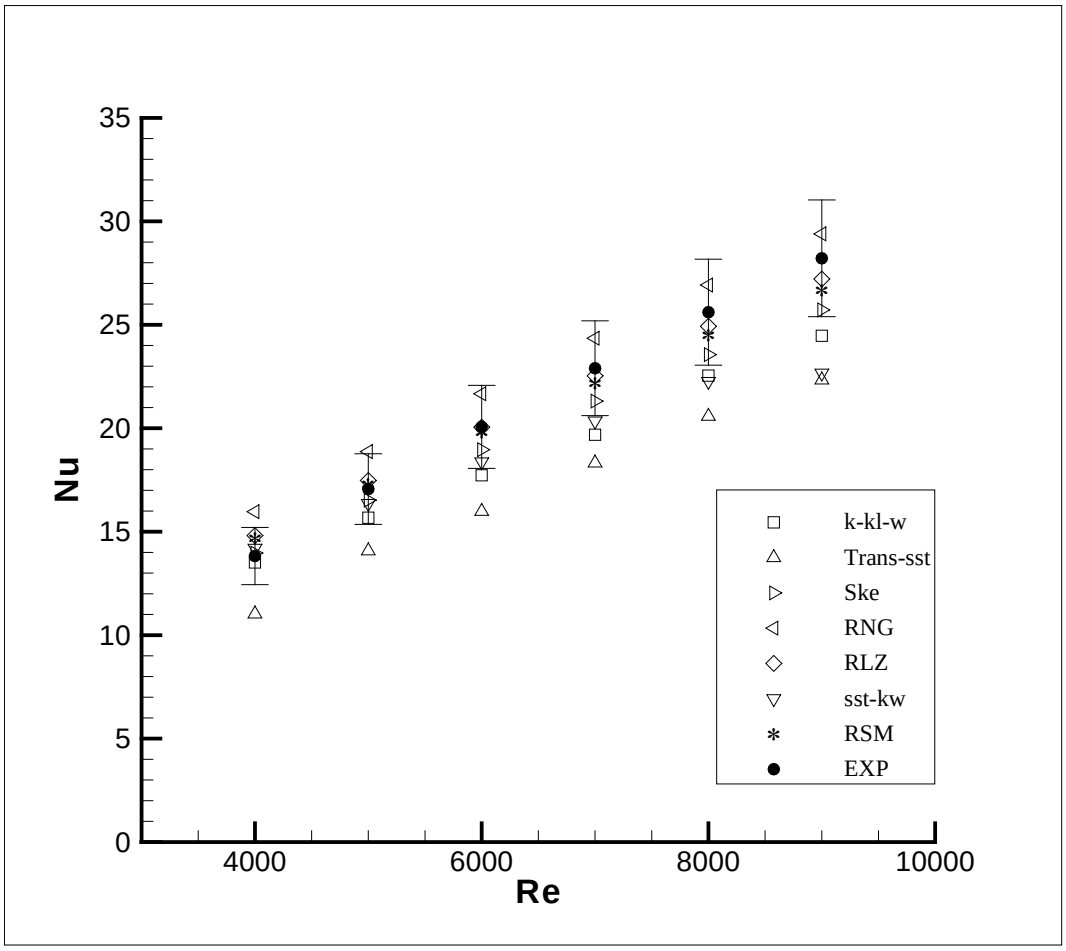

Fig.3 Predictions of periodic mean Nusselt numbers of a straight triangular duct with various turbulence models (the error bar is with ±10% of the correlated results)

Forced convection flow in a straight triangular duct is numerically simulated. Uniform wall temperature conditions were employed as thermal boundary conditions in the duct walls. Periodic boundary conditions were imposed in the flow direction. The comparisons of the Nusselt numbers between simulated and correlated results are shown in Figure 3, with Re between 4000 and 9000. Of the seven turbulence models employed, Ske, RLZ and RSM models plus enhanced wall treatment fit the correlation results well over the whole transition region. The deviations between simulations and correlations are all lower than 10%. RNG, sst-kw and k-kl-w models predict satisfactory Nu values in some of the cases, while the discrepancies between predictions and correlations can be larger than 10% in other comparisons. As shown from the figure, the Trans-sst model provides poorly prediction results compared with the correlations. The differences between the calculated and correlation results can be up to 21%. It seems

inappropriate to use Trans-sst model for the simulation of duct flow in transition region. Therefore, only Ske, RLZ, RNG, sst-kw, k-kl-w and RSM models are used for further evaluation.

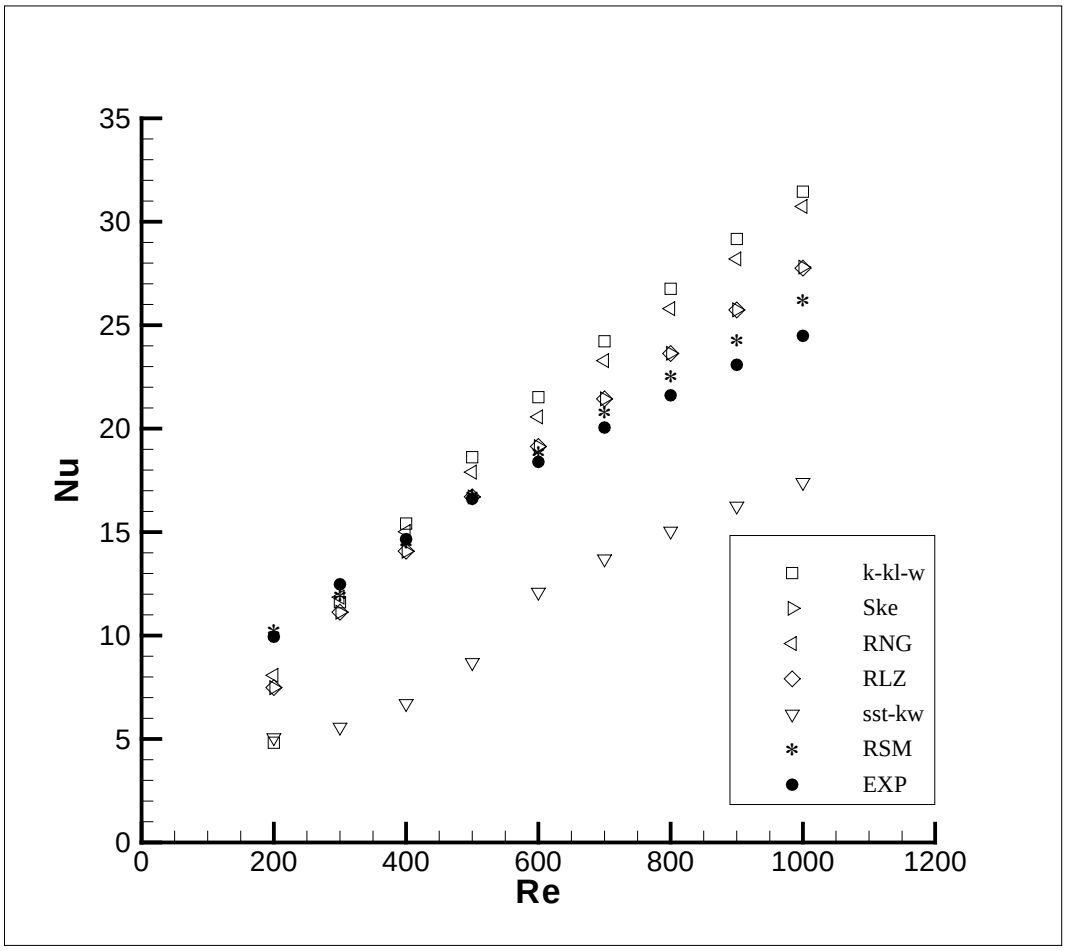

Fig.4 Predictions of periodic mean Nusselt numbers of a cross-corrugated triangular duct with various turbulence models

Further evaluation is performed through the comparisons between the predicted results and experimental data. A cross-corrugated triangular duct with geometric parameters identical to Scott and Lobato [5] is numerically simulated. The inclination angle of the channel is 90°, with $x_0 = 2mm$, $y_0 = 1mm$, $L_i = 2mm$. Figure 4 shows the comparisons between experimental results and the predictions of fully developed periodic mean Nusselt numbers with various turbulence models. Experimental data was obtained by the Scott's experiment using the heat-mass-transfer analogy [18] [19]. As shown from the figure, sst-kw significantly underpredicts the Nu values, and the discrepancies between predictions and experiments are over 30%. By using Ske and RLZ models, the CFD results and experimental data agree to within approximately 14%, except at the

Reynolds number of 200. Of the selected models, the RSM model fits the experiment the best. The overall behavior of the Nusselt number is predicted fairly well. The differences between simulated and experimental values are within 7%. By employing RSM model, the level of agreement between CFD and experiment presented here is considered good enough to provide comparative studies for different geometries, and thus is employed in the following investigations.

3.2 Geometric effect on heat transfer and pressure loss

A number of computations have been conducted to study the dependence of flow and heat transfer on geometrical parameters over Reynolds number ranges of 200-3000. As shown in Table 1, five different values of apex angles (30°, 60°, 90°, 120° and 150°) are considered under isosceles triangular cross-section channel. While two different values of sidewall angles (30° and 45°) with three different values of B/L (0.2, 0.4 and 0.6) are considered under isosceles trapezoidal cross-section channel. Note that the triangular channels are special cases of the trapezoidal channels with B/L=0. When the sidewall angle is 45° and B/L= 0, it becomes the triangular channel with Apex angle of 90°.

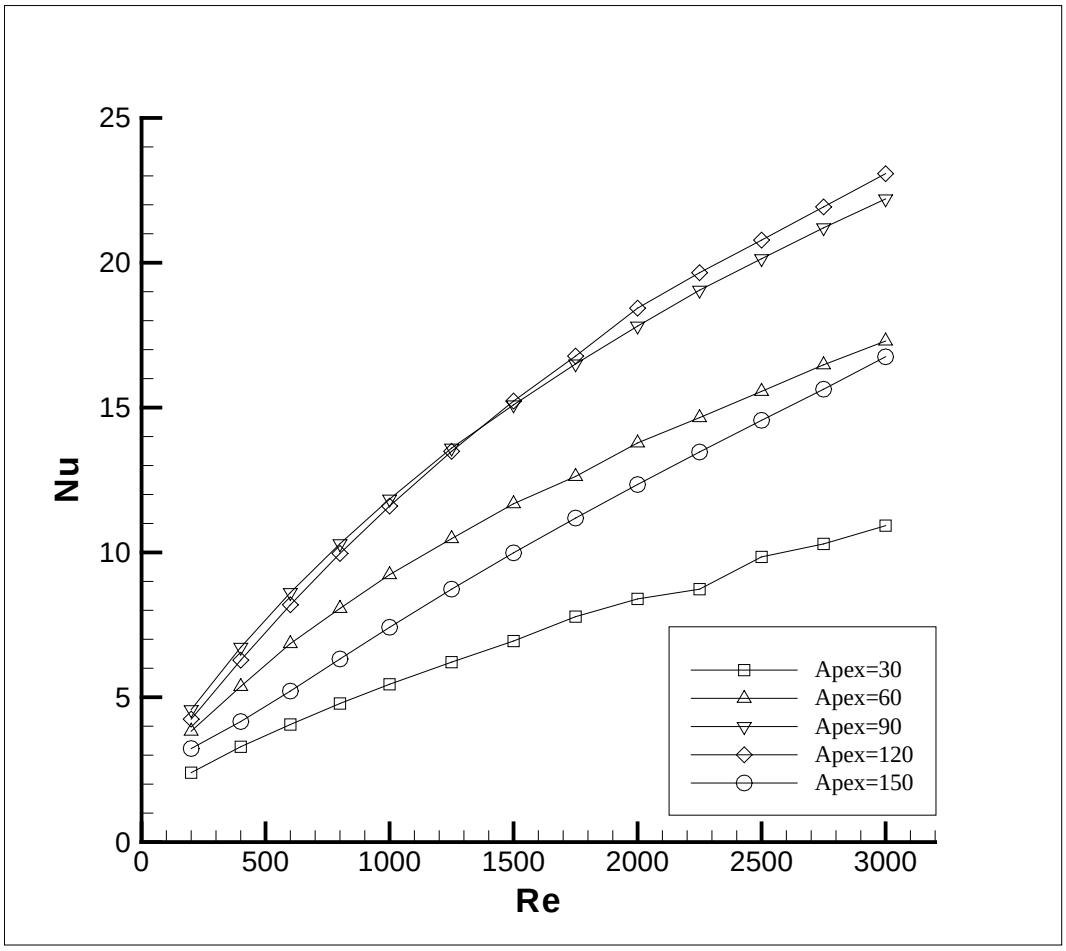

Fig.5 Periodic mean Nusselt numbers of a cross-corrugated triangular duct with different apex angles

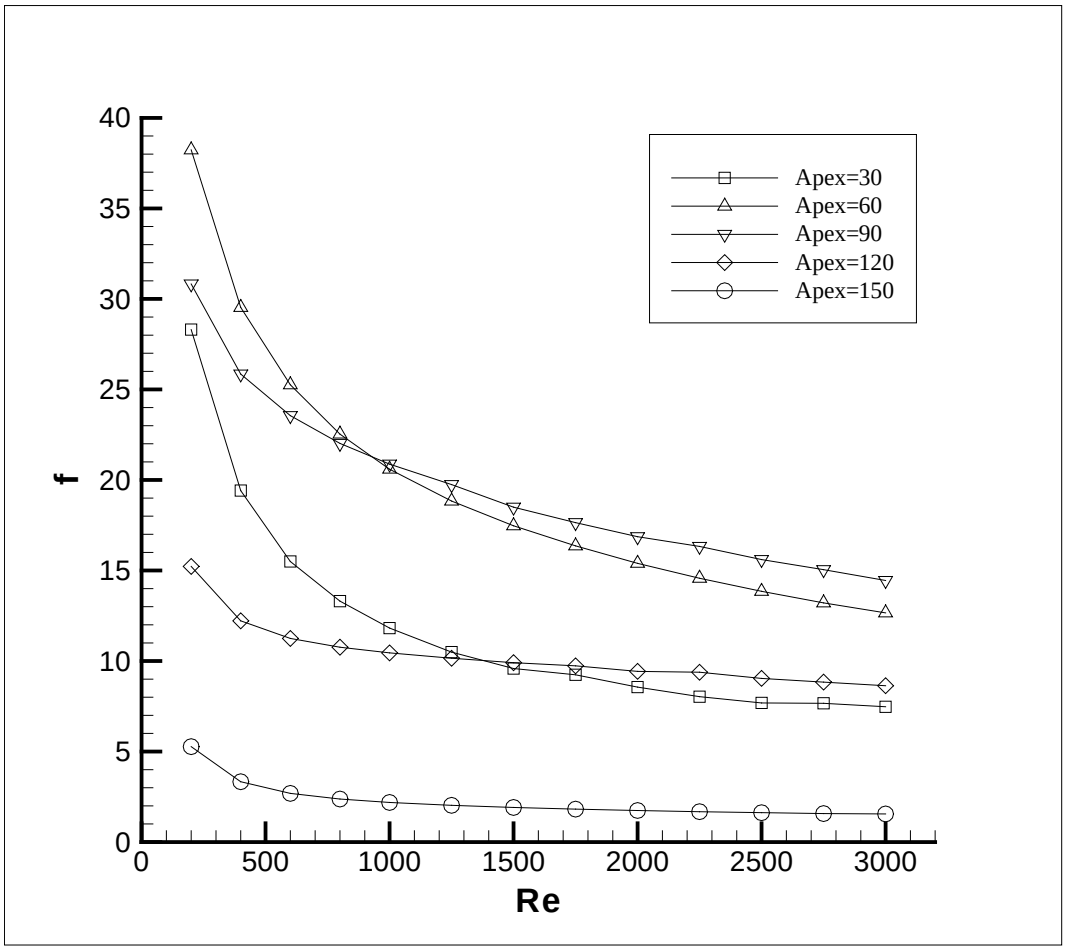

Fig. 6 Friction factors of a cross-corrugated triangular duct with different apex angles

Heat transfer and pressure drop are two key parameters to be considered in analyzing heat exchangers, and they are characterized by the Nusselt number (Nu) and the Fanning friction factor (*f*), respectively, in the current study. Figure 5-6 report the variation of Nu and *f* as a function of the Reynolds number under different Apex angles. The Nusselt numbers are increased with increasing Re numbers for all the geometries under consideration, while the friction factor are decreased. The results illustrate the influence of Apex angle on the heat transfer and pressure loss in a triangular cross-corrugated channel. Both Nu and *f* are strongly affected by this geometric parameter, but not vary linearly with the Apex angle. Comparing with other angles, the Apex angle of 30° provides the lowest Nu values under the same Reynolds numbers. At the 150° and 60° Apex angles, the Nusselt numbers are increased by 26%-54% and 58%-69%, respectively. The Nu values are of almost the same level when the Apex angles equal to 90° and 120°, with the differences lower than 7% over the studied Reynolds number range.

The maximum Nu values are obtained at the 90° and 120° Apex angles, which are generally two times of the values with Apex angle of 30°, implying the best heat transfer enhancement in the triangular channel with these angles. However, as shown in Figure 6, the friction factors under these two Apex angles are clearly different. When the Apex angle equals to 120°, the *f* values are of 47%-60% of that with Apex angle of 90°, indicating a substantially lower friction losses when Apex angle is 120°. The minimum *f* values are obtained at the 150° Apex angle under the same Reynolds number. The *f* values decrease with increasing Re for all the studied angles, while the gradient generally decreases as the Apex angle increases. When the Apex angle is 150°, the *f* values decrease more gently than that of other angles.

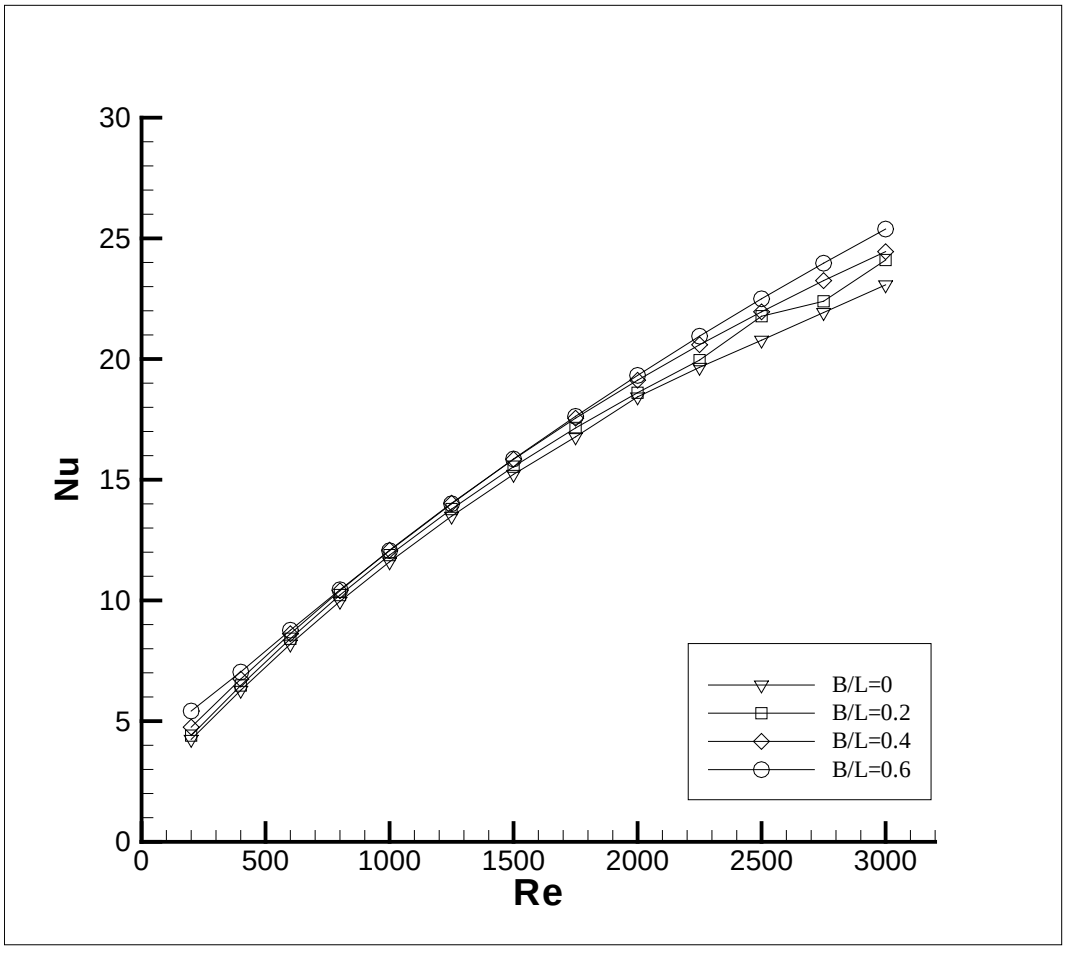

Fig.7 Periodic mean Nusselt numbers of a cross-corrugated duct with different aspect ratios (Sidewall angle = 30°)

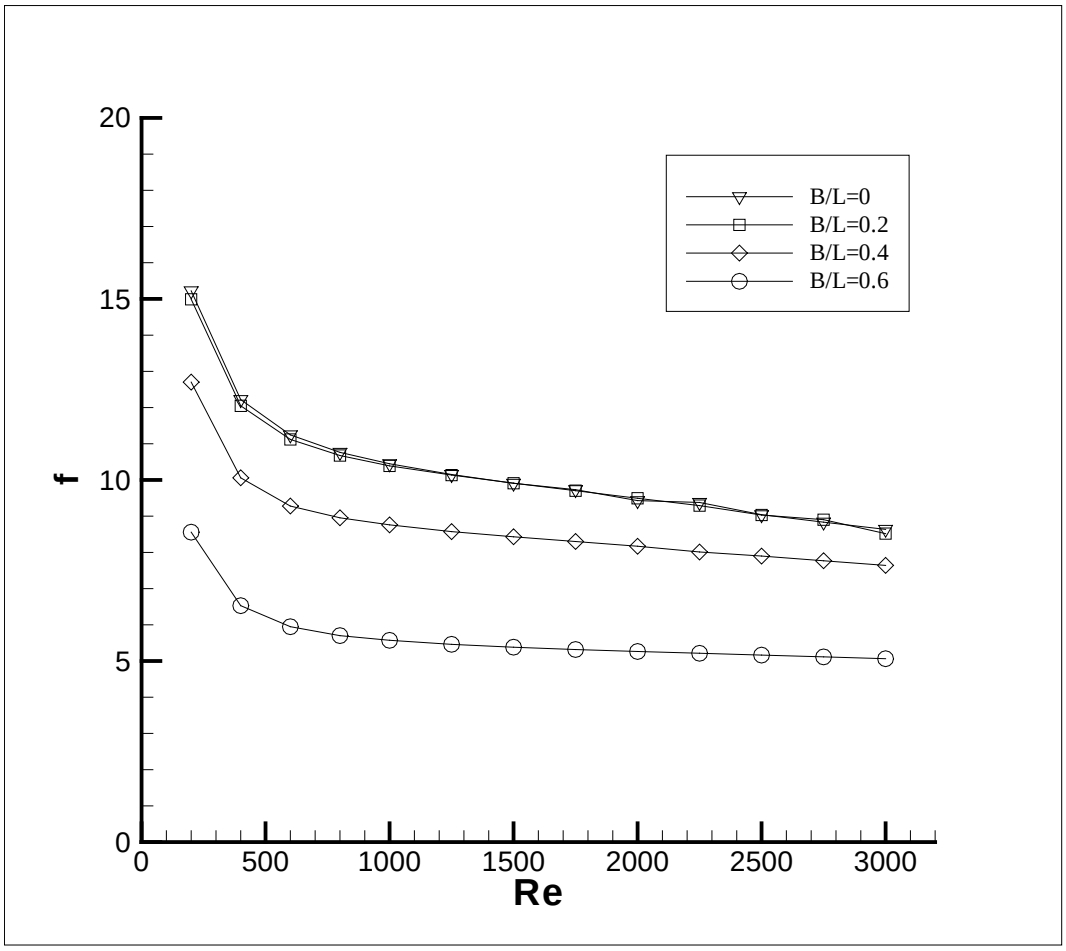

Fig.8 Friction factors of a cross-corrugated duct with different aspect ratios (Sidewall angle = 30°)

The effect of cross-sectional aspect ratio on heat transfer and friction loss in corrugated channel is illustrated in Figure 7-10. When the sidewall angle is 30°, the Nu and *f* values under various Reynolds numbers are shown in Figure 7-8 with different aspect ratios, while Figure 9-10 show the Nu and *f* values at the 45° sidewall angle. The correct trend that Nu increases with increasing Re is clear in the studied Re range for all the channels, while *f* decreases with increasing Re. Comparing with different aspect ratios, generally the maximum Nu values are obtained with B/L = 0.6 for both studied sidewall angles. And the *f* values are the lowest at this aspect ratio, indicating a lower pressure drop penalty comparing with other aspect ratios. As shown in Figure 7 and 9, changing B/L has relatively small influence on the heat transfer in the ducts. At the 30° sidewall angle, the differences of Nu values among different aspect ratios are less than 12%. For

the studied cases, the aspect ratio has a relatively greater impact on flow frictional loss, compared to its effect on the heat transfer.

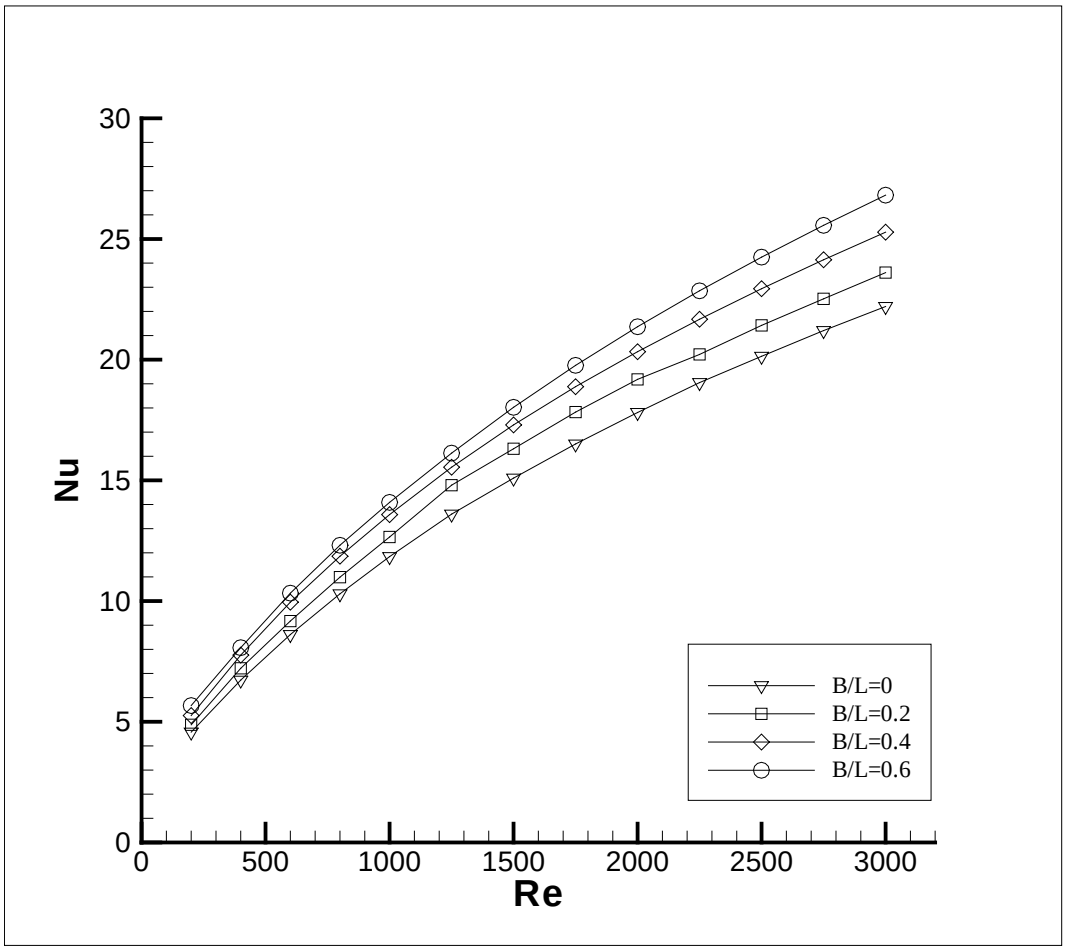

Fig.9 Periodic mean Nusselt numbers of a cross-corrugated duct with different aspect ratios (Sidewall angle = 45°)

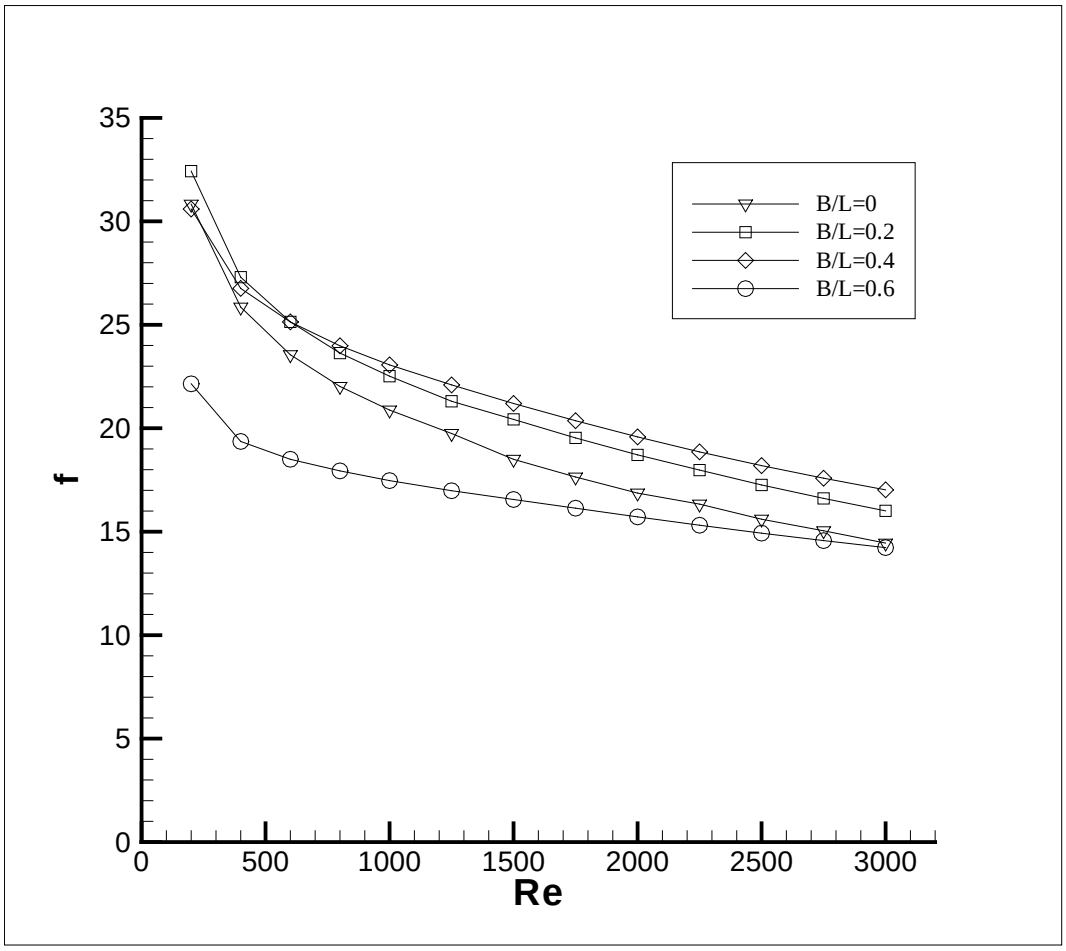

Fig.10 Friction factors of a cross-corrugated duct with different aspect ratios (Sidewall angle = 45°)

3.3 Performance evaluation

Considering that the improvements in heat transfer are always accompanied by increases in the frictional losses, it is necessary to evaluate the net enhancement obtained in different channels. One way of assessing the relative thermal-hydraulic performance enhancement is to consider the area goodness factor. This factor is defined as the ratio of the Colburn factor to friction factor (j/f), which establishes a relation between friction and heat transfer [39]. The measure seeks to evaluate the free-flow area (and hence the frontal area) requirements of a heat exchanger. It is a useful parameter when comparing surfaces with different cross-sectional shapes, and is widely used for many comparative studies [17] [40-42]. For a heat recovery application, high area goodness is required to minimize any increase in installed frontal area and hence drag.

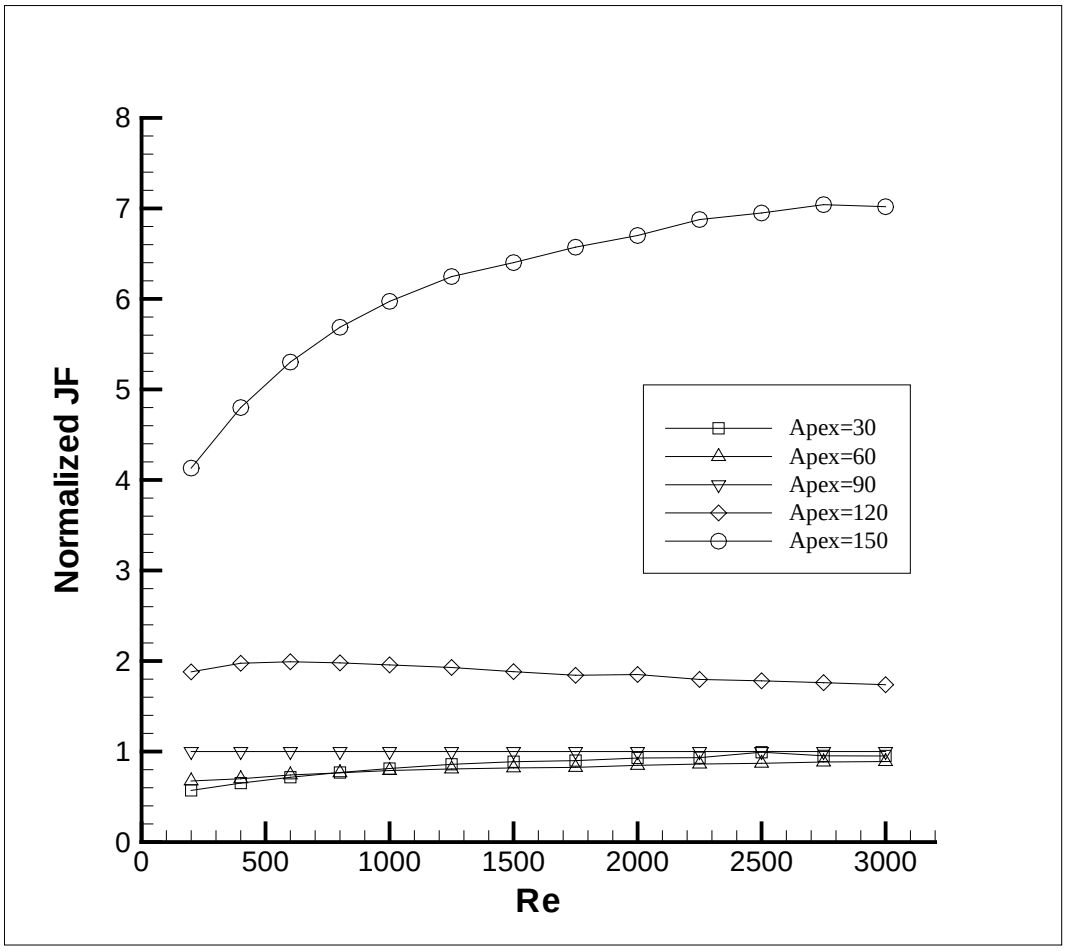

Fig.11 Normalized JF factor with different Apex angles

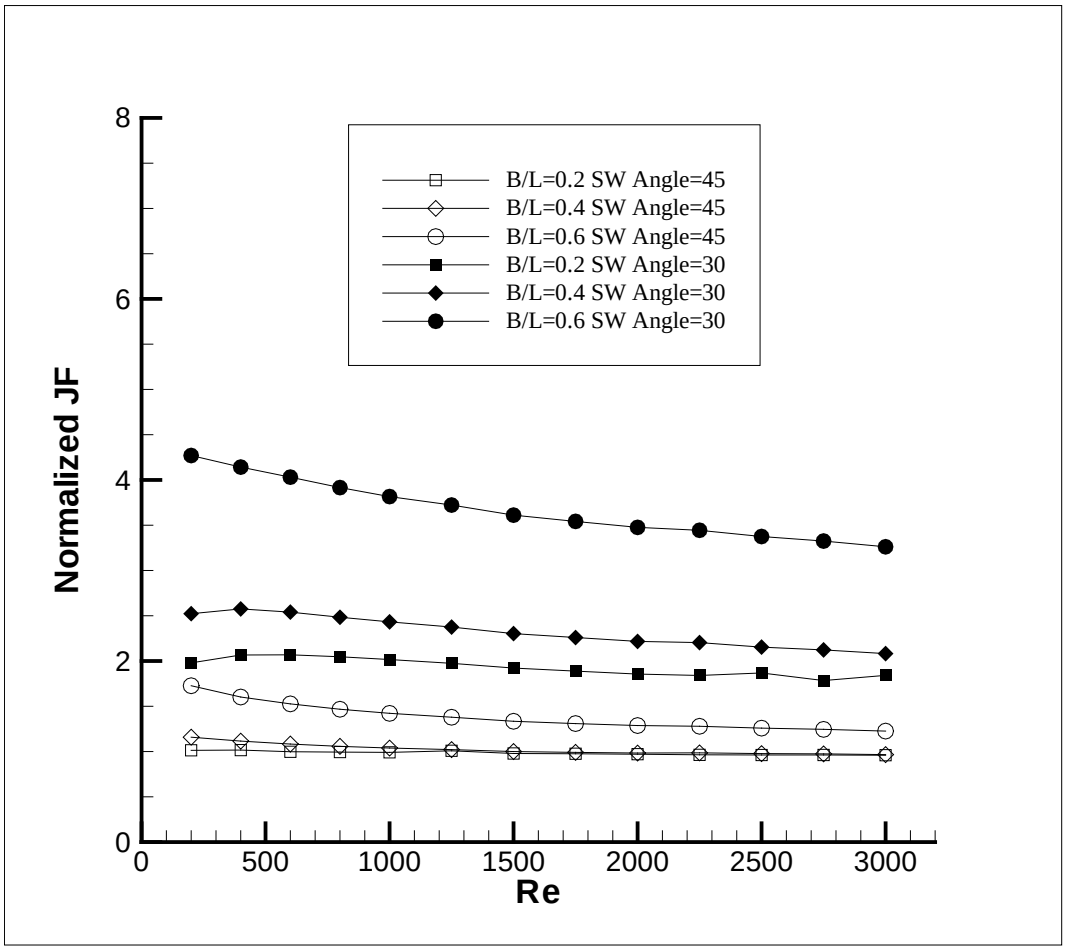

Fig.12 Normalized JF factor with different aspect ratios

Figure 11-12 show the variations of the normalized JF Factors ($(j/f)/(j_0/f_0)$) as a function of Reynolds number. The subscript (0) denotes the triangular cross-corrugated channel with Apex angle of 90°, which is the geometric shape used in Scott's experiments. As shown in Figure 11, when the Apex angles are 30°, 60° and 90°, the JF values are similar under the same Reynolds number. Substantial performance enhancement is observed at the 150° Apex angle, and the JF values are improved by 4-7 times comparing with the values at the 90° Apex angle. With regard to the aspect ratio effect, B/L=0.6 provides the greatest advantage under both studied sidewall angles, due to the maximum heat transfer capability with the lowest pressure penalty at this aspect ratio.

4. Conclusions

Simulations show the Apex angle of a triangular cross-corrugated channel strongly influences the thermohydraulic characteristics in the channel. The highest heat transfer capabilities in the triangular channel are obtained at the 90° and 120° Apex angles, and the periodic mean Nu values are generally two times of the minimum values when the Apex angle is 30° under the same Reynolds number. Thus the cross-corrugated triangular channels with these Apex angles are recommended for the purpose of heat transfer augmentation. With regard to the cross-sectional aspect ratio effect, for the studied cases, the aspect ratio has a relatively greater impact on flow frictional loss, compared to its effect on the heat transfer. The results also show that cross-sectional shapes influence the thermal-hydraulic performance in the channels. Generally the cross-corrugated triangular duct with the Apex angle of 150° offers the greatest performance enhancement over all the studied channels. The JF factor is enhanced by 4.1 to 7.0 times that in a triangular channel with Apex angle of 90°.

Acknowledgement

The research is funded by NSFC/RGC Joint Research project (3-ZG82).

References:

[1] W.M. Kays, A.L. London, Compact Heat Exchangers, 3rd Edition, McGraw-Hill, New York 1984.

[2] L. Z. Zhang and J. L. Niu, Effectiveness correlations for heat and moisture transfer processes in an enthalpy exchanger with membrane cores, ASME Journal of Heat Transfer 122 (2002) 922–929.

[3] L.Z. Zhang, Coupled heat and mass transfer through asymmetric porous membranes with finger-like macrovoids structure, International Journal of Heat and Mass Transfer 52 (2009) 751–759.

[4] L.Z. Zhang, F. Xiao, Simultaneous heat and moisture transfer through a composite supported liquid membrane, International Journal of Heat and Mass Transfer 51 (2008) 2179–2189.

[5] K. Scott and J. Lobato, Mass transport in cross-corrugated membranes and the influence of TiO2 for separation processes, Industrial & Engineering Chemistry Research 42 (2003) 5697–5701.
[6] L.Z. Zhang, Turbulent three-dimensional air flow and heat transfer in a crosscorrugated triangular duct, ASME Journal of Heat Transfer 127 (2005)1151–1158.

[7] W.W. Focke, J. Zachariades, I. Olivier, The effect of the corrugation inclination angle on the thermohydraulic performance of plate heat exchangers, International Journal of Heat and Mass Transfer 28 (1985) 1469–1497.
[8] J. Stasiek, M.W. Collins, M. Ciofalo, P.E, Chew, Investigation of flow and heat transfer in corrugated passages—I. Experimental results, International Journal of Heat and Mass Transfer 39 (1) (1996) 149–164.

[9] A. Muley, R.M. Manglik. Experimental study of turbulent flow heat transfer and pressure drop in a plate heat exchanger with chevron plates. ASME Journal of Heat Transfer 121 (1999) 110–117
[10] C. Zimmerer, P. Gschwind, G. Gaiser, V. Kottke, Comparison of heat and mass transfer in different heat exchanger geometries with corrugated walls, Experimental Thermal and Fluid Science 26 (2002) 269–273.
[11] M. Ciofalo, J. Stasiek, M.W. Collins. Investigation of flow and heat transfer in corrugated passages—II. Numerical simulations. International Journal of Heat and Mass Transfer 39 (1996) 165–192.
[12] M.A. Mehrabian, R. Poulter, Hydrodynamics and thermal characteristics of corrugated channels: computational approach, Applied Mathematical Modeling 24 (2000) 343–364.
[13] A.G. Kanaris, A.A. Mouza, S.V. Paras, Flow and heat transfer in narrow channels with corrugated walls: a CFD code application, Chemical Engineering Research & Design 83 (2005) 460-468.

[14] L. Zhang, D. Che, Influence of corrugation profile on the thermalhydraulic performance of cross-corrugated plates, Numerical Heat Transfer, Part A– Applications 59 (2011) 267–296.

[15] W. Han, K. Saleh, V. Aute, G. Ding, Y. Hwang, R. Radermacher, Numerical simulation and optimization of single-phase turbulent flow in chevron-type plate heat exchanger with sinusoidal corrugations, HVAC and R Research 17 (2011) 186–197.

[16] Y.C.Tsai, F.B. Liu, PT, Shen, Investigations of the pressure drop and flow distribution in a chevron-type plate heat exchanger, International Communications in Heat and Mass Transfer 36 (2009) 574-578.

[17] H.M. Metwally, R.M. Manglik, Enhanced heat transfer due to curvature-induced lateral vortices in laminar flows in sinusoidal corrugated-plate channels, International Journal of Heat and Mass Transfer 47 (10–11) (2004) 2283–2292.

[18] L.Z. Zhang, Convective mass transport in cross-corrugated membrane exchangers, Journal of Membrane Science 260 (2005) 75–83.

[19] J.H. Doo, M.Y. Ha, J.K. Min, R. Stieger, A. Rolt, C. Son, An investigation of cross-corrugated heat exchanger primary surfaces for advanced intercooled-cycle aero engines (Part-I: Novel geometry of primary surface), International Journal of Heat and Mass Transfer 55 (2012) 5256–5267.

[20] R.K. Shah, A.L. London, Laminar Flow Forced Convection in Ducts. Academic Press Inc., New York (1978) 223–246.

[21] Z. Zheng, D.F. Fletcher, B.S. Haynes, Laminar heat transfer simulations for periodic zigzag semicircular channels: chaotic advection and geometric effects, International Journal of Heat and Mass Transfer 62 (2013) 391–401.

[22] C.W. Leung, S.D. Probert, Forced-convective turbulent-flows through horizontal ducts with isosceles-triangular internal cross-sections, Applied Energy 57 (1997) 13–24.

[23] S. Chen, T.L. Chan, C.W. Leung, B. Yu, Numerical prediction of laminar forced convection in triangular ducts with unstructured triangular grid method, Numerical Heat Transfer, Part A–Applications 38 (2000) 209–224.

[24] R. Gupta, P.E. Geyer, D. F. Fletcher, B. S. Haynes, Thermohydraulic performance of a periodic trapezoidal channel with a triangular cross-section, International Journal of Heat and Mass Transfer 51 (2008) 2925–2929.

[25] H.Y Wu, Ping Cheng, Friction factors in smooth trapezoidal silicon microchannels with different aspect ratios, International Journal of Heat and Mass Transfer 46 (2003) 2519–2525.

[26] J. P. McHale, Suresh V. Garimella, Heat transfer in trapezoidal microchannels of various aspect ratios, International Journal of Heat and Mass Transfer 53 (2010) 365–375.

[27] L. C. Yang, M. Faghri, Y. Asako and Y. Yamaguchi, Numerical Prediction of Transitional Characteristics of Flow and Heat Transfer in a Corrugated Duct, ASME Journal of Heat Transfer 119 (1997) 62-69.

[28] L. Z. Zhang, Numerical study of periodically fully developed flow and heat transfer in cross-corrugated triangular channels in transitional flow regime, Numerical Heat Transfer, Part A-Applications 48 (2005) 387-405.

[29] S.V. Patankar, C.H. Liu, E.M. Sparrow. Fully developed flow and heat transfer in ducts having streamwise-periodic variations of cross-sectional area. ASME Journal of Heat Transfer 99 (1977) 180–186.

[30] B. E. Launder, D.B. Spalding, The Numerical Computation of Turbulent Flows, Computer Methods in Applied Mechanics and Engineering 3 (1974) 269-289.

[31] V. Yakhot, S.A. Orszag, S. Thangam, T.B. Gatski, C.G. Speziale, Development of turbulence models for shear flows by a double expansion technique, Physics of Fluids A-Fluid Dynamics 4 (1992) 1510-1520.

[32] T.H. Shih, W.W. Liou, A. Shabbir, Z. Yang, J. Zhu, A New $k-\varepsilon$ Eddy-Viscosity Model for High Reynolds Number Turbulent Flows - Model Development and Validation, Computers & Fluids 24 (1995) 227-238.

[33] F. R. Menter, R. B. Langtry, S. R. Likki, Y. B. Suzen, P. G. Huang, and S. Volker. A Correlation Based Transition Model Using Local Variables Part 1 - Model Formulation. In: ASME-GT2004-53452, ASME TURBO EXPO 2004, Vienna, Austria (2004).

[34] D. K. Walters, D. Cokljat, A three-equation eddy-viscosity model for reynolds-averaged navier-stokes simulations of transitional flows, Journal of Fluids Engineering, 130 (2008) 121401-14.

[35] F. R. Menter, Two-Equation Eddy-Viscosity Turbulence Models for Engineering Applications, AIAA Journal., 32 (1994) 1598–1605.

[36] B. E. Launder, Second-Moment Closure and Its Use in Modeling Turbulent Industrial Flows. International Journal for Numerical Methods in Fluids 9 (1989) 963–985.

[37] ANSYS FLUENT 13.0 Documentation. Canonburg, PA: ANSYS. ANSYS Inc. 2010.

[38] T. L. Bergman, A. S. Lavine, F. P. Incropera, D. P. DeWitt, Fundamentals of Heat and Mass Transfer, 7th Edition, John Wiley & Sons, Inc.; (March 21, 2011).

[39] A. L. London, Compact heat exchangers, Part 2, Surface geometry. Mechanical Engineering, 86 (1964) 31–34.

[40] Y. Islamoglu, C. Parmaksizoglu, The effect of channel height on the enhanced heat transfer characteristics in a corrugated heat exchanger channel, Applied Thermal Engineering 23 (2003) 979–987.

[41] E.A.M. Elshafei, M.M. Awad, E. El-Negiry, A.G. Ali, Heat transfer and pressure drop in corrugated channels, Energy 35 (2010) 101–110.

[42] Y.Wang, Y.L. He, D.H. Mei, W.Q. Tao, Optimization design of slotted fin by numerical simulation coupled with genetic algorithm, Applied Energy 88 (2011) 4441–4450.